Modified Topology of SEPIC Converter with High Gain Transfer Ratio for PV Applications

Abdelhakim BELKAID[a], Said Aissou[b], Slimane HADJI[a], Lylia LARBI[a]

belkaid08@yahoo.fr; said.aissou@univ-bejaia.dz; mail.hadji@gmail.com; lylia.larbi06@gmail.com

[a]*Laboratoire de Technologie Industrielle et de l'Information, Faculté de Technologie, Université de Bejaia, Bejaia 06000, Algeria*
[b]*Laboratoire de Maitrise Des énergies Renouvelables (LMER) Faculté de Technologie, Université de Bejaia, Bejaia, Algeria*

Received: 27.12.2024 Accepted:31.12.2024

***Abstract*—** This work introduced a modified SEPIC converter with a higher voltage conversion ratio. The configuration was achieved by simply adding passive electronic components—an inductor and a capacitor—to the conventional SEPIC converter. The output voltage generated by the power circuit, including the modified SEPIC, is higher compared to that of the conventional SEPIC, while maintaining the same duty cycle. Furthermore, the modified converter overcomes the parasitic effects of active and passive components in the circuit and produces reduced voltage and current ripples at its output. The modified SEPIC can be utilized in renewable energy power systems and industrial applications requiring high voltage levels.

Keywords—Photovoltaic applications; SEPICconverter; MPPT; High gain transfer ratio; modified DC-DC converter.

Nomenclature

I_{pv}	PV module current (A)
V_{pv}	PV module voltage (V)
N_s	number of series PV modules
N_p	number of parallel PV modules in
n_s	number of series PV cells connected in one string
R_s	PV module series resistance (Ω)
R_p	PV module parallel resistance (Ω)
a	the *p-n* junction ideality factor
P_{max}	Maximum power
V_{oc}	Open-circuit voltage
I_{sc}	Short-circuit current
V_{mpp}	Voltage at MPP
I_{mpp}	Current at MPP
k_v	Temperature coefficient of V_{oc}
k_i	Temperature coefficient of I_{sc}
f	Switching frequency
L	Inductor
C_1&C_2	Capacitors
R	Resistance
I_{ph}	The photo-current
I_s	The saturation current of the diode
v_t	the thermal voltage
k_b	the Boltzmann's constant
q	the charge of an electron
d	Duty cycle
u	switch position
V_o	Output voltage
MPPT	maximum power point tracking
Inc-Con	incremental conductance

1. Introduction

Global warming, rising energy demands, and the depletion of fossil fuels are significant concerns, prompting many countries to adopt renewable energy sources, such as photovoltaic (PV) panels, in their electric power systems. [1]. PV panels generate direct current (DC) electricity, usually at a low voltage ranging from 20 V to 40 V, whereas the grid operates at 220 V alternating current (AC). Therefore, a DC/DC stage is required to boost the voltage from approximately 20 V to 220 V. High gain power converters are necessary to solve the issue of low voltage and voltage level regulation [2-3]. Achieving a sufficient voltage level typically involves using a high duty cycle in usual boost converters or employing cascade converters [4]. However, this approach significantly impacts the competence and dependability of the power converter [5]. Various designs for this type of power converter have been proposed. DC/DC converters can broadly be classified into two categories: isolated and non-isolated topologies. Isolated DC/DC converters are commonly used to provide ground current isolation and to offer flexibility in voltage gain. However, they tend to be bulky and heavy due to the high-frequency transformer used in the DC/DC stage. Non-isolated DC/DC converters have gained significant attention due to their lower losses, smaller size, and reduced cost. Non-isolated topologies, like the boost converter, often face challenges with extreme duty ratio operation to achieve the required high voltage gain. The main challenge for non-isolated topologies is achieving high voltage gain while maintaining high efficiency. Several

advancements have been made to enhance the structure of DC/DC converters, aiming to achieve higher output voltages [6-7].

The converter described in [8] is designed by cascading two boost converters to achieve a higher voltage gain. This configuration consists of two boost converters with four power switches and their respective diodes, which substantially increases the hardware complexity. The converter proposed in [9] employs the voltage lift technique using two semiconductor switches to achieve a higher voltage gain. However, this approach can increase the converter size, and the output diode is subjected to higher voltage stress. The elevated voltage stress increases the risk of failure, potentially reducing the converter's lifespan. High voltage transfer ratio in converters has been accomplished using various techniques, including voltage multipliers [10-11], switched capacitance devices [12], switched inductance devices [13], mutual switched capacitor-inductor arrangements [14], and voltage lift methods [9,12,15-16]. However, these methods often suffer from increased hardware complexity and reduced efficiency. The converter developed in [17-18] uses two semiconductor switches and operates at a high duty ratio, which can lead to augmented overall power loss. Additionally, the power density of the converter is low. Hybrid-boost converters based on (Switched Capacitor & Voltage Multiplier Cell) and (Switched Capacitor & Switched Inductor) have been developed in [19] and [20-22], respectively. The increased component utilization in these converters results in a larger converter size. Additionally, both converters operate at a switching frequency of ≥100 kHz, which increases switching losses and the reverse recovery losses of the diodes. The converter developed in [20] integrates an active switched inductor, a passive switched inductor, a switched capacitor (SC) cell, and an auxiliary switch. The design employs three semiconductor switches, with a total component count of 16 to achieve the desired voltage gain. Consequently, the voltage gain to total component count (TCC) ratio is 0.68, which is relatively low. An extendable step-up DC-DC converter was developed in [21, 22] using multiple switched capacitor (SC) cells to enhance the voltage gain. The use of two SC cells results in a total component count (TCC) of 14 in [21], while the converter in [22] uses 16 components. Both converters employ five semiconductor switches, which increases the size and control complexity of the converter during closed-loop operation. The modified SEPIC converter in [23] uses 10 components, with two semiconductor switches and three inductors occupying more space than other components in the circuit. Additionally, the converter was tested at a great duty cycle (D = 0.7) to attain a voltage gain of 7.9, which is relatively low. The converters developed in [24-25] use coupled inductors to get a high voltage ratio. However, incorporating coupled inductors in the design can increase the converter size and reduce its power density. Converters developed in [26] and [27] use switched capacitors (SC) and voltage multiplier cells (VMCs) to achieve a high voltage gain. However, the use of 16 components in these designs increases the size of the converter. In [28], the developed converter employs three switches and three inductors, potentially increasing its size. Additionally, the voltage stress on the switches (S2, S3) and diodes (D0) is high, which may elevate the risk of failure. In [29], a combined topology of the interleaved boost converter and voltage multiplier cell (VMC) has been developed to achieve a higher voltage ratio. However, the use of 16 components may lower the ratio of voltage gain to total component count (TCC) and reduce the power density of the converter.

In this article, a non isolated converter is developed to achieve a higher output voltage with a lower duty ratio, addressing the aforementioned drawbacks

In this work, a modified SEPIC converter is proposed, incorporating a single additional inductor and capacitor into the conventional design. This modification enhances the output voltage level while minimizing output power oscillations. As a result, the converter transitions from a voltage step-up/down configuration to a high voltage gain step-up converter.

A comparative analysis with the conventional structure is presented by applying incremental conductance MPPT control to both converters. Simulation results are provided to demonstrate the enhanced performance of the proposed design.

2. PV Panel Modeling

The simple PV system seen in Fig. 1, is composed by PV panel, a DC/DC converter, MPPT control, and a DC load.

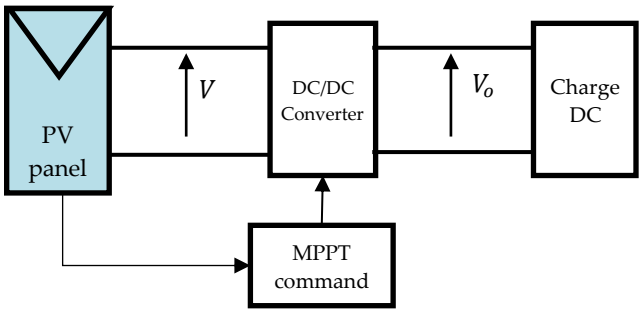

Fig. 1. Simple PV system

A. Model of the PV cell

In this work, a single diode cell model is used as depicted in Figure 2 [4-5].

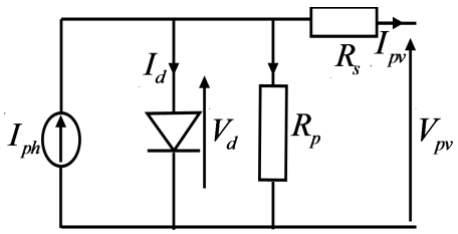

Fig. 2. Equivalent circuit of a PV cell

The output current is expressed as the next equation [6]:

$$I_{pv} = I_{ph} - I_s \left[exp\left(\frac{q\left(V_{pv} + R_s I_{pv}\right)}{a\, k_b T} \right) - 1 \right] - \frac{V_{pv} + R_s I_{pv}}{R_p} \quad (1)$$

B. Incremental Conductance control

This method is the second most widely used after P&O, offering ease of implementation while addressing the divergence issue of P&O during rapid changes in sunlight intensity [7]. It operates by comparing conductance with the rate of change in conductance, as illustrated in Figure 3.

The product between the voltage and the current give the power of the solar panel:

$$P = V.I \quad (2)$$

And the derivative of the power will be as:

$$\frac{dP}{dV} = \frac{d(VI)}{dV} = V.\frac{dI}{dV} + I = V.\frac{\Delta I}{\Delta V} + I \quad (3)$$

At the peak of the curve, we can make:

$$\frac{\Delta P}{\Delta V} \approx 0 \Longrightarrow \frac{\Delta I}{\Delta V} \approx -\frac{I}{V} \quad (4)$$

So, the MPP can be attained by comparison the conductance G and the increment of the conductance dG. We can mark:

If $\frac{\Delta I}{\Delta V} > -\frac{I}{V}$, left of the MPP →Increase V (5)

If $\frac{\Delta I}{\Delta V} < -\frac{I}{V}$, right of MPP →Decrease V (6)

If $\frac{\Delta I}{\Delta V} \approx -\frac{I}{V}$, close to the PPM (7)

The Incremental method offers high-quality performance even beneath a rapid change in climate conditions, but it suffers from complex and very expensive control circuit.

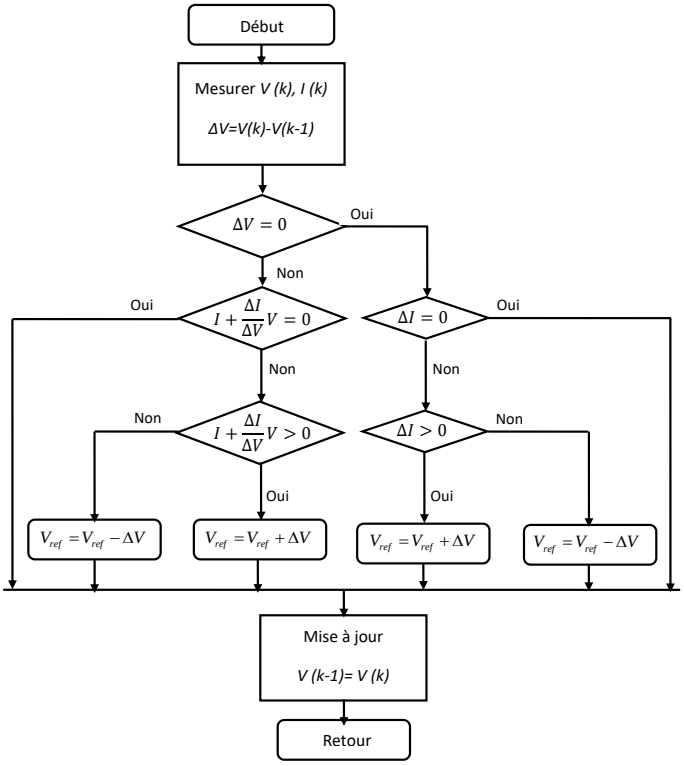

Fig. 3. The Incremental method flowchart

3. Modified Topology of Sepic Converter

A. *Fundamental SEPIC structure*

The structure of the basic SEPIC converter is given on the Figure 6 as mentioned in [8]. The load voltage can be superior or inferior to the input voltage [9].

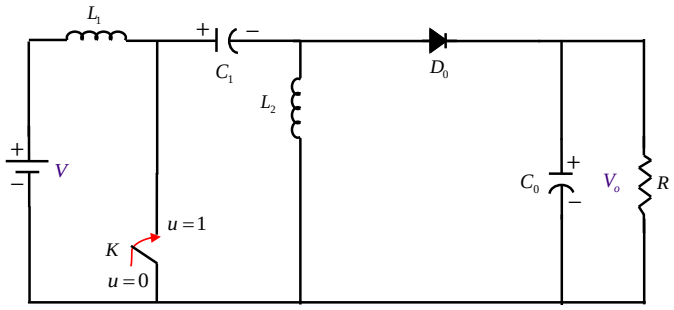

Fig. 4. Fundamental SEPIC structure

Two modes describe the function of the converter:

The first is when the switch K is closed ($0 < t < \alpha T$), the SEPIC structure becomes as in Fig. 5:

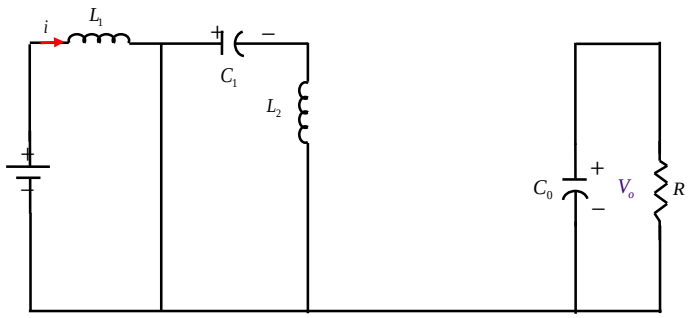

Fig. 5. Fundamental SEPIC structure, mode ON

Through this mode T_{on}, the inductances currents increase linearly and the energy is stored in L_1. The capacitor C_0 supplied the load.

In this mode, the voltages across the inductors L_1 and L_2 can be given by:

$$V_{L_1} = V \quad (8)$$

$$V_{L_2} = -V_{C_1} \quad (9)$$

The second mode is when the switch K is opened $\alpha T < t < T$. The corresponding circuit of the SEPIC will be as shown in Figure 6.

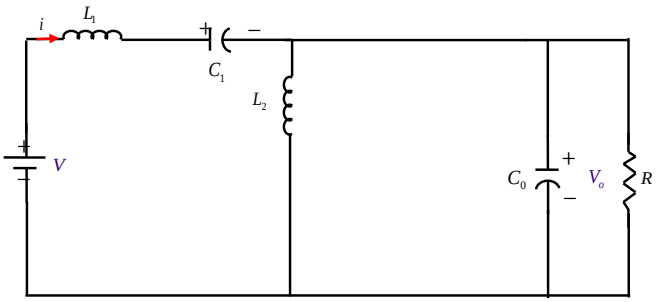

Fig. 6. Fundamental SEPIC structure, mode OFF

The diode D begins to conduct. The currents of the inductors L_1 and L_2linearly decrease and their sum flows through the diode towards the load, where a part of the energy is consumed by the load and another part is stored in the capacitor C_0.

The voltages on the inductors are:

$$V_{L_1} = V - V_o - V_{C_1} \quad (10)$$

$$V_{L_2} = V_o \quad (11)$$

In steady state, the average value of the voltage on the inductance is null, so we can write:

$$\alpha \cdot V_{L(on)} + (1-\alpha) \cdot V_{L(off)} = 0 \quad (12)$$

If we apply this principle to L_1 and L_2, we will have:

$$\alpha \cdot V + (1-\alpha) \cdot (V - V_o - V_{C_1}) = 0 \quad (13)$$

$$\alpha(-V_{C_1}) + (1-\alpha)V_o = 0 \quad (14)$$

From the last two equations, we find that:

$$\frac{V_o}{V} = \frac{\alpha}{1-\alpha} \quad (15)$$

which means the converter operates as a step-down converter (if $\alpha < 0.5$); or step-up converter(if $\alpha > 0.5$).

B. The modified topology of the SEPIC converter

By adding one inductor and one capacitor to the basic structure, we get the proposed SEPIC shown in Figure 7.

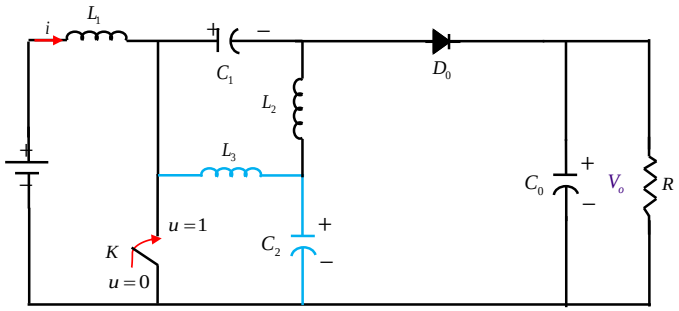

Fig. 7. Modified structure of the SEPIC converter

During the first operating sequence (T_{on}), the switch K is closed and the diode is blocked, the converter equivalent circuit becomes as shown on Fig. 8

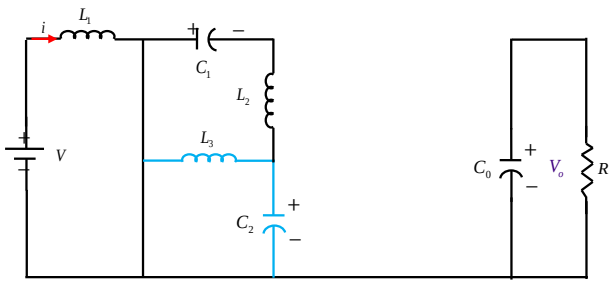

Fig. 8. Modified SEPIC structure, mode ON

The equations of this phase can be given below:

$$V_{L_1} = V. \quad (16)$$

$$V_{L_2} = -V_{C_1} - V_{C_2} \quad (17)$$

$$V_{L_3} = -V_{C_2}. \quad (18)$$

During the second phase (T_{off}), the switch is opened. The converter equivalent circuit becomes:

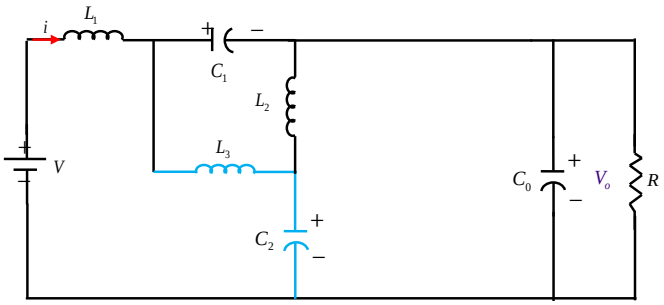

Fig. 9. Modified SEPIC structure, mode OFF

The equations of voltages across the inductors are given below:

$$V_{L_1} = V - V_o - V_{C_1} \quad (19)$$

$$V_{L_2} = V_o - V_{C_2}. \quad (20)$$

$$V_{L_3} = V_o + V_{C_1} - V_{C_2} \quad (21)$$

In steady state, the average value of the voltage on the inductance is equal to zero, so we can write:

$$\alpha \cdot V + (1-\alpha) \cdot (V - V_o - V_{C_1}) = 0 \quad (22)$$

$$-\alpha(V_{C_1} + V_{C_2}) + (1-\alpha)(V_o - V_{C_2}) = 0 \quad (23)$$

$$\alpha(-V_{C_2}) + (1-\alpha)(V_o + V_{C_1} - V_{C_2}) = 0 \quad (24)$$

or:

$$V = (1-\alpha)V_o + (1-\alpha)V_{C_1} \quad (25)$$

$$V_{C_2} = (1-\alpha)\,V_o - \alpha V_{C_1} \quad (26)$$

$$V_{C_2} = (1-\alpha)V_o + (1-\alpha)V_{C_1} \quad (27)$$

thus:

$$V_{C_2} = V_{C_2} + V_{C_1} \Rightarrow V_{C_1} = 0 \quad (28)$$

So, Eq. 25 becomes:

$$V = (1-\alpha)V_o \quad (29)$$

And the voltage transfer ratio of the customized SEPIC is given by:

$$\frac{V_o}{V} = \frac{1}{1-\alpha} \quad (30)$$

This equation proves that the modified structure allows the SEPIC converter to become a boost with high amplifier ratio (bigger than 10).

4. Simulation Results

Modified structure of the SEPIC converter was numerically tested using MATLAB/Simulink software.

The different specifications used in the tests are given in table 1.

TABLE I. DIFFERENT SPECIFICATIONS USED IN SIMULATION.

Setting	Value
P_{max}	60W
V_{oc}	21.1V
I_{sc}	3.8A
V_{mpp}	17.1V
I_{mpp}	3.5A
k_v	-0.08 V/°C
k_i	0.003 A/°C
f	10kHz
C	20µF
C_1	1000µF
C_2	1000µF
C_0	470µF
L_1	5mH
L_2	5 MHz
R	30Ω

For the first test of simulation, we kept the irradiance fixed at 1000 W/m^2 and we varied the temperature. The tests were made for duration of 2.8 s, and the corresponding results are drawn in Fig. 10**.** The curves of PV current $\boldsymbol{I_{pv}(A)}$, voltage $\boldsymbol{V_{pv}(V)}$, power $\boldsymbol{P_{pv}(W)}$ and output voltage $\boldsymbol{V_o(V)}$ are presented.

For the second test, we kept the temperature fixed at 25 °C and we varied the irradiance. The corresponding results are drawn in Fig. 11

The waveforms of $\boldsymbol{V_{pv}(V)}$ and $\boldsymbol{P_{pv}(W)}$ are inversely proportional to temperature variations, while $\boldsymbol{I_{pv}(A)}$ is only minimally affected.

The results indicate that the various parameters closely align with the PV characteristics under constant solar irradiance. Notably, the waveforms of current $\boldsymbol{I_{pv}(A)}$ and power $\boldsymbol{P_{pv}(W)}$ are significantly influenced by changes in sunlight, whereas $\boldsymbol{V_{pv}(V)}$ is only slightly affected. Furthermore, a comparison between $\boldsymbol{V_{pv}(V)}$ $\boldsymbol{V_o(V)}$ confirms that the employed converter is a step up voltage kind.

Below standard test conditions (STC), the solar module produces an average of 59.9 W of power, 17.3 V of voltage, and 3.4 A of current. However, when the irradiance level decreases to 500 W/m^2, these values drop to an average of 29 W of power, 17.2 V of voltage, and 1.7 A of current.

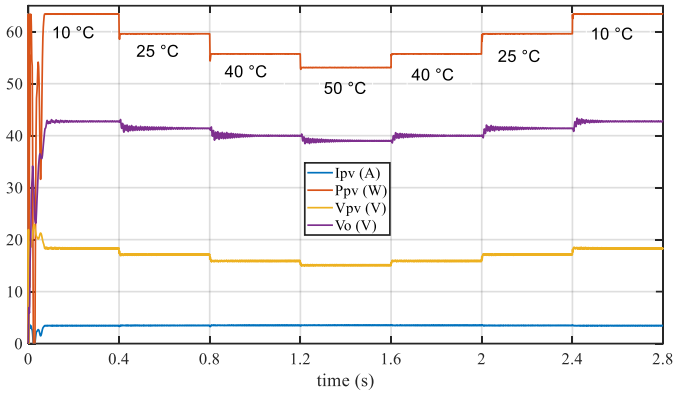

Fig. 10. Results of simulation with temperature change and fixed irradiance

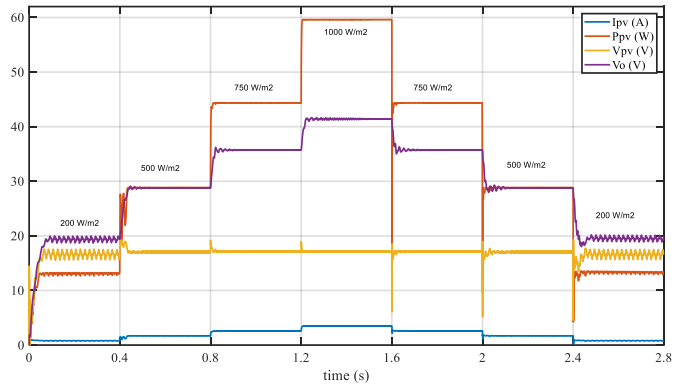

Fig. 17. Results of simulation with irradiance change and fixed temperature.

We can clearly see more stability with the modified structure than the classical one, with the proposed SEPIC structure less power oscillation level is obtained.

5. Conclusion

This paper presents a modified SEPIC converter with an improved voltage conversion ratio. The modification is achieved by integrating simple passive components (an inductor and a capacitor) into the traditional SEPIC converter design. The resulting configuration generates a higher output voltage compared to the conventional SEPIC converter, while maintaining the same duty cycle. In addition, the modified converter mitigates the parasitic effects of the active and passive components in the circuit, thereby effectively reducing the voltage and current ripples at the output. The modified SEPIC converter is well suited for renewable energy systems and industrial applications requiring high voltage levels. Moreover, its minimal component count helps reduce costs and improve overall efficiency.

References

[1] M. Abbasi, “Using dynamic thermal rating and energy storage systems technologies simultaneously for optimal integration and utilization of renewable energy sources”. Int. J. Eng. Sci. 33(1), 92–104 (2020).

[2] R. Rajesh, N. Prabaharan, “Design of New Nonisolated High Gain Converter for Higher Power Density”. Int. Trans. Electr. Energy Syst. 2023, 2023, 2011926.

[3] Qun Qi, Davood Ghaderi, M. Guerrero Josep, “Sliding mode controller-based switched-capacitor-based high DC

gain and low voltage stress DC-DC boost converter for photovoltaic applications", International Journal of Electrical Power & Energy Systems, Volume 125, 2021, 106496, https://doi.org/10.1016/j.ijepes.2020.106496.

[4] M. Lotfi Nejad, B. Poorali, E. Adib, A. A. Motie Birjandi, "New Cascade Boost Converter with Reduced Losses". IET Power Electron. 2016, 9, 1213–1219.

[5] H. Hidalgo, R. Orosco, H. Huerta, N. Vázquez, C. Hernández, S. Pinto, "A High-Voltage-Gain DC–DC Boost Converter with Zero-Ripple Input Current for Renewable Applications". Energies 2023, 16, 4860. https://doi.org/10.3390/en16134860.

[6] A. Amir, A. Amir, H. S. Che, A. Elkhateb, N. A., Rahim, "Comparative analysis of high voltage gain dc–dc converter topologies for photovoltaic systems". Renew. Energy 136, 1147–1163 (2019)

[7] M. Abbasi, "A new transformer-less step-up DC–DC converter with high voltage gain and reduced voltage stress on switched-capacitors and power switches for renewable energy source applications". IET Power Electron. 14, 1347–1359 (2021). https://doi.org/10.1049/pel2.12106

[8] H. Ardi, A. Ajami, F. Kardan, S.N. Avilagh, "Analysis and implementation of a nonisolated bidirectional DC–DC converter with high voltage gain", IEEE Trans. Ind. Electron. 63 (8) (2016) 4878–4888, http://dx.doi.org/10.1109/TIE.2016. 2552139.

[9] A. Rajabi, A. Rajaei, V. M. Tehrani, P. Dehghanian, J. M. Guerrero, B. Khan, "A non-isolated high step-up dc–dc converter using voltage lift technique: analysis, design, and implementation". IEEE Access 10, 6338–6347 (2022)

[10] S. Mahdizadeh, H. Gholizadeh, R. S. Shahrivar, E. Afjei, A. Mosallanejad, "An ultra high step-up dc–dc converter based on vmc, posllc, and boost converter". IET Power Electron. 15(10), 901–918 (2022).

[11] V. S. Rao, K. Sundaramoorthy, "Performance analysis of voltage multiplier coupled cascaded boost converter with solar pv integration for dc microgrid application". IEEE Trans. Ind. Appl. 59(1), 1013–1023 (2022)

[12] S. M. Alilou, M. Maalandish, A. Samadian, P. Abolhassani, S. H. Hosseini, M. H. Khooban, "A new high step-up dc–dc converter using voltage lift techniques suitable for renewable applications". CSEE J. Power Energy Syst. (2023).

[13] Y. Wang, Q. Bian, X. Hu, Y. Guan, D. Xu, "A high-performance impedance-source converter with switched inductor, IEEE Trans". Power Electron. 34 (4) (2019) 3384–3396, http://dx.doi.org/10.1109/TPEL.2018.2853581.

[14] M. A. Salvador, T. B. Lazzarin, R. F. Coelho, "High step-up DC–DC converter with active switched-inductor and passive switched-capacitor networks", IEEE Trans. Ind. Electron. 65 (7) (2018) 5644–5654, http://dx.doi.org/10.1109/TIE.2017. 2782239.

[15] S. Khan, M. Zaid, M. D. Siddique, A. Iqbal, "Ultra high gain step up dc/dc converter based on switched inductor and improved voltage lift technique for high-voltage applications". IET Power Electron. 15(10), 932–952 (2022)

[16] M. A. Bhupathi Kumar, V. Krishnasamy, "Enhanced quadratic boost converter based on voltage lift technique for fuel cell powered electric vehicle". Comput. Electr. Eng. 102, 108256 (2022)

[17] S. Gopinathan, V. S. Rao, K. Sundaramoorthy, "Family of non-isolated quadratic high gain dc–dc converters based on extended capacitor-diode network for renewable energy source integration". IEEE J. Emerg. Sel. Top. Power. Electron. 10(5), 6218–6230 (2022).

[18] L. Liu, D. Li, "Novel modified high step-up dc/dc converters with reduced switch voltage stress". Int. Trans. Electr. Energy Syst. 2022(7), 1–24 (2022).

[19] A. Manuel, S. S. Andrade, T. M. K. Faistel, R. A. Guisso, A. Toebe, "Hybrid high voltage gain transformerless dc–dc converter". IEEE Trans. Ind. Electron. 69(3), 2470–2479 (2021)

[20] J. Qi, X. Wu, S. He, W. Xu, J. Liu, "Investigation on the optimal operation and control strategy of a wide-range switched-capacitor/switchedinductor dc/dc converter". IET Power Electron. 16(2), 227–242 (2023)

[21] B. Faridpak, M. Bayat, M. Nasiri, R. Samanbakhsh, M. Farrokhifar, "Improved hybrid switched inductor/switched capacitor dc–dc converters". IEEE Trans. Power Electron. 36(3), 3053–3062 (2020)

[22] H. J. Farahani, M. Rezvanyvardom, A. Mirzaei, "Non-isolated high step-up dc–dc converter based on switched-inductor switched-capacitor network for photovoltaic application". IET Gener. Transm. Distrib. 17(3), 716–729 (2023)